5624 *Biochemistry* **2010,** *49,* 5624–5633
DOI: 10.1021/bi902164h

BIOCHEMISTRY
including biophysical chemistry & molecular biology
Article

Engineered Disulfide Bonds Restore Chaperone-like Function of DJ-1 Mutants Linked to Familial Parkinson's Disease[†]

Todd Logan,[§,||] Lindsay Clark,[§,‡] and Soumya S. Ray*[,§,‡,||]

[‡]*Harvard Center for Neurodegeneration and Repair and Department of Neurology, Harvard Medical School, Boston, Massachusetts 02115, and* [§]*Center for Neurologic Diseases, Brigham and Women's Hospital, Boston, Massachusetts 02115* [||] *These authors contributed equally to this work.*

Received December 17, 2009; Revised Manuscript Received June 7, 2010

ABSTRACT: Loss-of-function mutations such as L166P, A104T, and M26I in the DJ-1 gene (PARK7) have been linked to autosomal-recessive early onset Parkinson's disease (PD). Cellular and structural studies of the familial mutants suggest that these mutations may destabilize the dimeric structure. To look for common dynamical signatures among the DJ-1 mutants, short MD simulations of up to 1000 ps were conducted to identify the weakest region of the protein (residues 38−70). In an attempt to stabilize the protein, we mutated residue Val 51 to cysteine (V51C) to make a symmetry-related disulfide bridge with the preexisting Cys 53 on the opposite subunit. We found that the introduction of this disulfide linkage stabilized the mutants A104T and M26I against thermal denaturation, improved their ability to scavenge reactive oxygen species (ROS), and restored a chaperone-like function of blocking α-synuclein aggregation. The L166P mutant was far too unstable to be rescued by introduction of the V51C mutation. The results presented here point to the possible development of pharmacological chaperones, which may eventually lead to PD therapeutics.

Parkinson's disease (PD)[1] is a progressive neurodegenerative disease characterized by the loss of dopaminergic neurons from the substantia nigra *pars compacta*, and the presence of cytosolic inclusions known as Lewy bodies (*1*). These inclusions are rich in fibrils of α-synuclein and parkin. A more recently identified gene product of unknown function, DJ-1 (PARK7, location 1p36.2-3 on the human genome), has been implicated in autosomal-recessive early onset PD (*2*). Mutations in the DJ-1 gene include a 14 kb deletion encompassing the first six exons (*2*), as well as missense mutations encoding DJ-1 variants. L166P, one of the well-studied variants, appears to cause dramatic loss of stability leading to low cellular levels of protein (*3*, *4*). Other variants such M26I (*5*), E64D (*6*), and E163K (*7*) are also known to affect cellular levels of DJ-1 but to lesser extent compared to L166P. These homozygous mutations may trigger a loss of function, the presumed cause of their pathogenicity. Another variant A104T (*8*, *9*) was associated with PD patients in a heterozygous state, and structural analysis of the X-ray structure reveals local perturbations in the central β-sheet suggesting that mutation may lead to a loss of stability (*10*). Apart from the association of DJ-1 with recessive Parkinson's disease, DJ-1 has been implicated in pathogenesis of various types of cancer (*11*), may play a role in male fertility (*12*), and may reduce oxidative stress following stroke (*13*). Although the exact biochemical function of DJ-1 is not known, it has been shown to associate with transcription factors (*14*−*17*), bind RNA (*18*), and undergo SUMOylation (*19*). Furthermore, DJ-1 may have an overall effect on cell fate through its involvement in the PTEN/Akt signaling pathway (*20*). Wild-type DJ-1 has been shown to rescue α-synuclein aggregation in vitro, pointing toward a possible chaperone-like function (*21*−*23*). We demonstrate in this work that the mutations that lead to structural defects in DJ-1 may be restored to near wild-type-like stability and function by covalently reinforcing the weak parts of the protein with appropriately placed disulfide bridges.

DJ-1 is a dimeric member of the ThiJ/Php family of proteins with an α/β-fold homologous to the flavodoxin-like molecular chaperone Hsp31 (*24*, *25*). The oxidation of a key highly conserved residue, C106, results in an acidic PI shift, which may signal DJ-1 to translocate to the mitochondria (*26*). The translocation to mitochondria is believed to be neuroprotective in nature (*27*). It has been suggested that translocation of DJ-1 to the mitochondria may play an important role in mitochondrial autophagy (*28*), an important cellular process known to be compromised in age-related disorders such as PD (*29*, *30*). Cys 106 is surrounded by charged amino acids from both subunits of the protein, generating a unique chemical environment, suggesting the importance of a dimeric quaternary structure for normal protein function (*31*, *32*). In contrast to wild-type DJ-1, the PD-linked mutant L166P is highly destabilized, as judged by in vitro studies (*33*), the yeast two-hybrid system (*4*), and mammalian cells (*34*). While L166P causes severe structural defects, M26I was reported to be less stable than the wild type (WT) and to produce lower steady state levels in cell culture studies (*35*). A reduced dimer population was observed for A104T in cross-linking studies in cell culture systems but not in co-immunoprecipitation assays (*36*). X-ray crystallographic analysis indicates a loss of stability for M26I, A104T, and E163K (*10*), but they appear to

[†]This work was supported by the National Institutes of Health (Grants AG08476 and NS038375 to Peter T. Lansbury).

*To whom correspondence should be addressed. E-mail: sray@rics.bwh.harvard.edu. Phone: (617) 821-0955. Fax: (617) 768-8606.

[1]Abbreviations: PD, Parkinson's disease; ROS, reactive oxygen species; TTR, transthyretin; SOD, human superoxide dismutase-1; GST, glutathione *S*-transferase; CCD, charge-coupled detector; PBS, phosphate-buffered saline; MWCO, molecular weight cutoff; TBS, Tris-buffered saline (pH 7.4).

 Published on Web 06/08/2010

retain dimeric structure in solution. M26I disrupts the hydrophobic core; A104T causes packing defects in a critical β-sheet near the C-terminus, and E163K disrupts a structurally critical salt bridge.

The central hypothesis of this work is based on the notion that if the "weakest structural link" in a mutant protein structure can be identified, it may be reinforced with either a covalent bond, such as a disulfide linkage, or small molecules to prevent the subsequent downstream unfolding events. This strategy has been successfully applied to transthyretin (involved in familial amyloid polyneuropathy) (*37*) and SOD-1 (involved in ALS) (*38*), where simple stabilization of the native dimeric (SOD) or tetrameric (TTR) states with small molecules or disulfide bridges abolished aggregation (*37*, *39*). A 1000 ps MD simulation of L166P, M26I, and A104T revealed that the region of the protein consisting of residues 38−70 exhibited the most variation in motion when compared to WT DJ-1. This region was also observed to have a high degree of motion by experimental methods such as NMR conducted by Eliezer and co-workers (*40*) and X-ray crystallographic solvent mapping analysis conducted by Ringer and co-workers (*41*). L166P simulation studies conducted by Daggett and co-workers have also indicated this same region to be disrupted early in the simulation (*42*). In this work, we demonstrate that covalently reinforcing the dimer interface region with disulfide bonds can lead to increased protein stability, improved antioxidant function of the mutant protein, and promoted chaperone-like function in DJ-1 mutants. Though familial DJ-1 mutations represent a small class of PD-causing mutations, promoting or prolonging antiaggregation function of WT DJ-1 might help patients with various synucleinopathies.

MATERIALS AND METHODS

Protein Expression and Purification. Rosetta competent cells (Novagen) were transformed with pGEX GST fusion vectors (GE Healthcare) encoding wild-type DJ-1, as well as DJ-1^{L166P}, DJ-1^{M26I}, DJ-1^{V51C}, DJ-1$^{L166P/V51C}$, DJ-1$^{M26I/V51C}$, and DJ-1$^{V51C/A104T}$ variants of DJ-1 genes synthesized by DNA2.0 (https://www.dna20.com/) with codons optimized for expression in *Escherichia coli*. Cells were grown at 37 °C in LB broth containing 100 μg/mL ampicillin and 50 μg/mL chloramphenicol until the OD_{600} reached 0.4. Protein expression was initiated by addition of 750 μM isopropyl β-D-thiogalactopyranoside (IPTG) followed by incubation at 18 °C for 16 h. Cells were harvested by centrifugation and stored at −80 °C. Frozen cells resuspended in phosphate-buffered saline (PBS) (pH 7.4) and 400 mM KCl were lysed using a Microfluidizer (Microfluidics Corp.) and centrifuged at 20000*g* for 45 min. The supernatant was loaded using a peristaltic pump onto a GSTPrep FF16/10 column (GE Healthcare) that had been pre-equilibrated with 3 column volumes of PBS (pH 7.4) and 400 mM KCl. The GST column was washed with ~100 mL of PBS and 400 mM KCl, and protein was eluted with a solution containing 250 mM Tris-HCl (pH 7.4), 1.25 M NaCl, and 10 mM reduced L-glutathione. Eluate was combined with 500u Prescission Protease (GE Healthcare) and dialyzed overnight against PBS (pH 7.4), 400 mM KCl, and 1 mM DTT to cleave the GST tag. The GST tag was removed when the cut protein was passed back over the same column. Flow-through fractions were analyzed by SDS−PAGE, concentrated using Centiprep YM-10 centrifugal filter devices (Amicon) to a final volume of ~10 mL, and further purified by size exclusion chromatrography on a Superdex 75 gel filtration column (GE Healthcare). Collected fractions were analyzed by SDS−PAGE and adjusted to a final concentration of ~4 mg/mL. The protein samples were dialyzed extensively against 50 mM Tris buffer (pH 8.0) with a minimum of three buffer changes. The extensive dialysis induced disulfide bond formation in DJ-1^{V51C}, DJ-1$^{L166P/V51C}$, DJ-1$^{M26I/V51C}$, and DJ-1$^{V51C/A104T}$ variants by air oxidation but not oxidation of C106 as judged by mass spectrometric analysis. Complete oxidation of Cys 106 was induced by incubating the protein with 0.1% H_2O_2 for 1 h prior to its use in the α-synuclein aggregation assay but not for the glutathione peroxidase assay (described below). MALDI mass spectrometry was conducted to determine accurate molecular masses as well as assess the oxidation state of Cys 106.

Molecular Dynamics Simulation. The initial protein structures for DJ-1^{WT} [Protein Data Bank (PDB) entry 1pdv], DJ-1^{M26I} (PDB entry 2rk4), and DJ-1^{A104T} (PDB entry 2rk3) were downloaded (http://www.rcsb.org/pdb) and examined to add all the missing side chains to generate a model suitable for simulation studies. The familial DJ-1 mutation L166P (no structure available) was modeled using PYMOL. Following addition of hydrogen at all the relevant positions, the resulting structures were energy-minimized to remove any geometric strains that might have been introduced as a result of the modeling procedure. His residues were protonated at Nδ2 except His 138 was protonated at Nδ1. Tautomer assignments for His residues were based on the investigation of likely hydrogen bonds in the crystal structure. GROMACS version 3.2 (*43*) using the GROMOS96 force field was chosen for all the subsequent steps in the simulation procedure. The protein structures were enclosed in a cubic box and filled with water molecules such that the waters extended 5 Å from the protein molecule. Energy calculations were conducted using periodic boundary conditions, and calculations of electrostatic energy were conducted using particle mesh Ewald (PME) summations and a nonbonded cutoff at 10 Å. The simulation overall involved five major steps: (1) energy minimization of the system in 500 steps of the steepest descent followed by 500 steps of conjugate gradient energy minimization at a constant volume, (2) restrained molecular dynamics for 10 ps at 300 K while freezing the position of the protein and the ions and moving only the solvent, (3) warming the whole system for 10 ps to 300 K at a constant volume using new, random velocities, and (4) 1 ns MD of the whole system at a constant temperature of 500 K and a constant pressure of 1 atm after prewarming of the system to 700 K for 20 ps. The generation of a control trajectory at 300 K for WT DJ-1 was conducted in a similar fashion. Snapshots of the structures were saved every 2 ps during the trajectories. The simulations were undertaken on a Beowulf cluster using eight-node 3.0 GHz Xeon processors configured in dual processor nodes (16 CPU total). The resulting coordinates were analyzed using G_RMSF from the GROMACS (*43*) software suite.

Glutathione Peroxidase Assay for DJ-1 Autoxidation. A glutathione peroxidase assay kit (Cayman Chemical) was used to measure the peroxidase activity of DJ-1. Protein samples were diluted to a final concentration of 100 μM in assay buffer [50 mM Tris-HCl (pH 7.6) and 5 mM EDTA] and a substrate mixture containing NADPH, glutathione, and glutathione reductase. Reactions were initiated by addition of cumene hydroperoxide, and absorbance was monitored at 340 nm using a SpectraMax Plus plate reader (Molecular Devices). All samples were normalized to the activity of a glutathione peroxidase (100 nM) positive control (provided by Cayman Chemicals). Data points were averaged over five independent experimental measurements.

Differential Scanning Fluorimetry using ThermoFluor. Solutions of 7.5 μL of 100× Sypro Orange (Invitrogen) and 10 μM protein were added to the wells of a 96-well thin-wall PCR plate (Bio-Rad). The plates were sealed with Optical-Quality Sealing Tape (Bio-Rad) and heated in an iCycler iQ5 Real Time PCR Detection System (Bio-Rad) from 4 to 90 °C in increments of 0.5 °C. Fluorescence changes in the wells of the plate were monitored simultaneously with a charge-coupled device (CCD) camera. The wavelengths for excitation and emission were 490 and 575 nm, respectively. For each protein sample, data from three independent wells were averaged and plotted.

α-*Synuclein Fibrillation Assay*. Fibril formation was monitored using a ThioT assay. Samples of α-synuclein were dissolved in 50 mM Tris-HCl (pH 8.0) and filtered through a Millipore Microcon 100K MWCO filter. The final concentration in the reaction mixture was adjusted to 75 μM; 75 μM amounts of DJ-1^{WT} or the mutants (preincubated with 0.1% H_2O_2) were added to α-synuclein and preincubated over ice for 30 min prior to aggregation. In cases of control experiments, where the effect of reducing the disulfide bond in DJ-$1^{M26I/V51C}$ and DJ-$1^{V51C/A104T}$ on α-synuclein aggregation was explored, the protein right after purification was dialyzed overnight with 10 mM DTT to ensure all cysteine residues were in free thiol form. Mass spectrometric analysis revealed that Cys 106 was in thiol form in these protein samples. Aggregation was initiated by incubation of the samples at 37 °C with constant stirring with a mini-stirring bar; 10 μL samples of the aggregating mixture were withdrawn at regular intervals and assayed for fibril content by monitoring ThioT fluorescence. Data from five independent aggregation assays for α-synuclein incubated with various forms of DJ-1 were used for generation of the data plot and error bars. Thio-T (Sigma) was filtered through a 0.2 μm polyether sulfone filter and added to the sample wells (384-well format plate) at a final concentration of 20 μM and incubated for 1 min prior to the recording of fluorescence. Samples were mixed by agitation for 60 s at 120 rpm. Fluorescence enhancement was monitored at 490 nm by an Analyst 96-384 plate reader (LJL Biosystems).

Electron Microscopy Analysis. Samples of α-synuclein, DJ-1, and mixtures of α-synuclein and DJ-1 were diluted 6-fold with TBS prior to adsorption to glow-discharged, carbon-coated copper grids. Grids were washed with four drops of buffer and stained with two drops of freshly prepared 0.75% (w/v) uranyl formate (Pfaltz&Bauer, Waterbury, CT). Specimens were inspected with a JEOL 1200EX electron microscope operated at 80 kV, and images were recorded at a nominal magnification of 40000 using low-dose procedures.

Analytical Size Exclusion Chromatography. All chromatography was performed in TBS (20 mM Tris and 150 mM NaCl) (pH 7.4) on a Waters 2690 Alliance HPLC or Agilent 1100 series HPLC system and monitored at 276 nm. Protein samples were spun at 13000*g* prior to injection on the column.

RESULTS

Structural Changes in the Familial Mutants DJ-1^{L166P}, DJ-1^{A104T}, and DJ-1^{M26I} Probed by MD Simulation. Familial DJ-1 mutants are distributed all over various secondary structural elements on the protein structure (Figure 1a) and appear to have a wide range of effects on protein folding and stability. The central hypothesis behind this investigation is based on the notion that covalent tethering of protein residues using disulfide bonds in the most facile region should be able to improve the overall stability of the mutant and possibly restore wild-type-like function (*44*−*46*). It was therefore useful to conduct MD simulations of the various DJ-1 mutants and compare them with each other and DJ-1^{WT} to look for a common dynamical signature. Daggett and co-workers (*42*) have conducted simulation studies on DJ-1^{L166P} and shown destabilization near the dimer interface regions. In this section, we have extended the studies to other familial DJ-1 mutants to Parkinson's disease. Short molecular dynamics simulations were conducted on DJ-1^{WT} (PDB entry 1pdv), DJ-1^{M26I} (PDB entry 1rk4), and DJ-1^{A104T} (PDB entry 1rk3) at 700 K using GROMACS (*43*) for a total of 1000 ps (1 ns) in the presence of water molecules. Because there is no crystal structure for L166P, the mutation was modeled into DJ-1^{WT} (PDB entry 1pdv) and simulated under the conditions described above. The Cα atom root-mean-square deviation (rmsd) from the crystal structure was calculated for all of the snapshots from each residue to give an approximate idea of the degree of structural perturbation during the course of the simulation (Figure 2a). The control trajectory for WT DJ-1 at 300 K shows a < 1.5 Å deviation from the initial crystal structure, suggesting that the system remains stable at room temperature. The familial mutants, DJ-1^{L166P}, DJ-1^{A104T}, and DJ-1^{M26I}, when simulated at 700 K showed increased mobility and perturbation from the initial model. The mutants DJ-1^{L166P} and DJ-1^{A104T} showed a greater degree of perturbation than DJ-1^{M26I} under identical simulation conditions. The majority of the root-mean-square deviation (rmsd) from the initial structure could be ascribed to motions around the N- and C-termini of the protein, the regions of residues 38−70 and 127−138 (Figure 2a). Solvent-exposed helix 6 between residues 127 and 138 shows the highest degree of perturbation from the initial structures and appears to be the most mobile region of the protein. Though this region shows a high rmsd, it appears to be a common region of high mobility between the WT and the mutants. This is therefore likely to be a natural protein motion and not induced entirely by mutation. It is currently not possible to deduce the precise origin of this motion from the short simulation studies. Similar observations of natural protein motions versus mutation induced motions have been made in simulation studies conducted with other protein systems (*47*).

The region of residues 38−70 in the control trajectory (WT at 300 K) and WT at 700 K exhibited less motion when compared to the familial mutants. When the motion was mapped on the crystal structures of M26I, A104T, and the L166P model, this region of highest perturbation coincided with parts of the dimer interface of DJ-1 (Figure 2b shown for DJ-1^{A104T}) near the β3 and β4 strand regions. A large motion was also observed in helix B (numbering scheme adapted from ref *48*). Among the three mutants, M26I exhibited the smallest amount of motion relative to the WT protein around residues 38−70. It is noteworthy that this region is located ∼21 Å from the A104T mutation site, 17 Å from M26I, and 25 Å from L166P, suggesting long-range coupling between the mutation site and the region of residues 38−70 (Figure 2a and Supplemental Figure 1a of the Supporting Information). Similar observations have been made in the case of other proteins as well (*47*). The motion in the Cys 106 region does not appear to be much different between WT and the mutants in this short simulation study. However, we cannot rule out larger motions in this region in longer simulation studies.

Intersubunit Disulfide Bonds in the Facile Region Stabilize Familial PD-Linked Mutant DJ-1 against Thermal Denaturation. Though a detailed analysis of the simulation trajectory has not been conducted in this study, preliminary

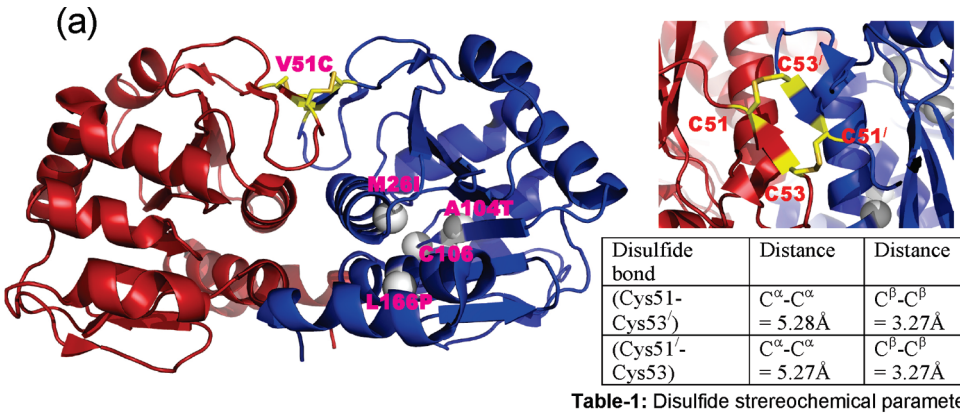

Disulfide bond	Distance	Distance	Torsion
(Cys51-Cys53′)	C^{α}-C^{α} = 5.28Å	C^{β}-C^{β} = 3.27Å	χ = 89.54°
(Cys51′-Cys53)	C^{α}-C^{α} = 5.27Å	C^{β}-C^{β} = 3.27Å	χ = 89.24°

Table-1: Disulfide strereochemical parameters for V51C

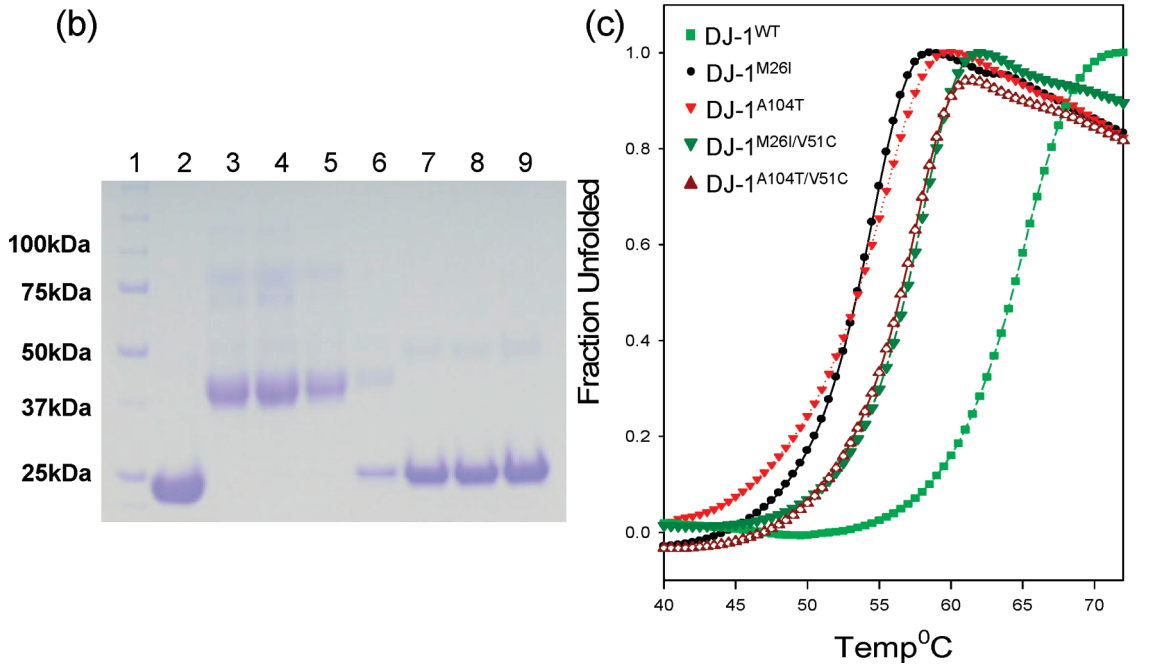

FIGURE 1: (a) Ribbon representation of the two subunits of DJ-1 showing the positions of the various familial Parkinson's disease-causing mutations and the disulfide linkages (side panel) used in this investigation. The table lists the stereochemical parameters for the disulfide bonds generated as a result of the V51C mutation. (b) Gradient (from 4 to 12%) SDS−PAGE analysis of disulfide bond formation in DJ-1^{V51C}, DJ-$1^{L166P/V51C}$, DJ-$1^{M26I/V51C}$, and DJ-$1^{V51C/A104T}$ under nonreducing conditions. Lane 1 contained molecular weight markers and lane 2 DJ-1^{WT}. Lanes 3−6 contained DJ-1^{V51C}, DJ-$1^{M26I/V51C}$, DJ-$1^{A104T/V51C}$, and DJ-$1^{L166P/V51C}$, respectively, under nonreducing conditions. Lanes 7−9 contained DJ-1^{V51C}, DJ-$1^{M26I/V51C}$, and DJ-$1^{A104T/V51C}$, respectively, under reducing conditions. (c) Thermal melting curves (fluorescence) for DJ-1^{WT} and various mutants measured using ThermoFluor (Sypro Orange) on a real-time PCR machine. Thermal melting curves for each protein sample were measured from three independent wells (n = 3), and the averaged data are shown here. The melting curves indicate that DJ-1^{WT} is the most stable with a T_m of 65 ± 0.5 °C. The familial mutants were found to be less stable than WT with DJ-1^{M26I} (T_m = 52 ± 0.5 °C) and DJ-1^{A104T} (T_m = 53 ± 0.5 °C). The V51C disulfide-linked versions of the mutant DJ-1 were more stable compared to the familial mutants (DJ-$1^{M26I/V51C}$ T_m = 57 ± 0.5 °C, and DJ-$1^{A104T/V51C}$ T_m = 58 ± 0.5 °C).

analysis suggests that the region of residues 38−70 of mutant DJ-1 is one of the most facile regions (maximum rmsd). It may be hypothesized that covalently reinforcing this region using disulfide bridges should lead to overall stabilization of the protein. On the basis of DSDESIGN (*49*) disulfide modeling, it was concluded that the V51 → C51 mutation (V51C) would result in a pair of symmetry-related disulfide bridges with C53 on the opposite subunit with near-optimal stereochemistry (Figure 1a). Mere proximity of cysteine residues is not sufficient to induce disulfide bond formation [stereochemical parameters are critical (*49*); see the table in Figure 1]. The V51C mutation was introduced into the L166P, M26I, and A104T familial DJ-1 variants. The double mutants DJ-$1^{A104T/V51C}$, DJ-$1^{L166P/V51C}$, and DJ-$1^{M26I/V51C}$ and DJ-1^{V51C} were purified, and following air oxidation to generate the disulfide bridges between the native cysteine (C53) and the introduced cysteine (V51C), the protein samples were analyzed via SDS−PAGE under nonreducing conditions (Figure 1b). In contrast to protein harboring the familial mutations alone, the oxidized versions of the double mutants bearing the V51C mutation migrated as an ~42 kDa band (Figure 1b; more than 90% of the protein migrated as a dimer), indicating that the engineered cysteine residues resulted in a covalently cross-linked dimeric form of DJ-1. The DJ-$1^{L166P/V51C}$ mutant failed to migrate as a dimer in our SDS−PAGE analysis. This finding is in agreement with it being an extreme destabilizing mutation probably leading to loss of quaternary and tertiary protein structure.

Following oxidation, the thermal stability of the various mutants was measured using ThermoFluor (differential scanning fluorimetry) on a PCR machine with real-time optics (details in

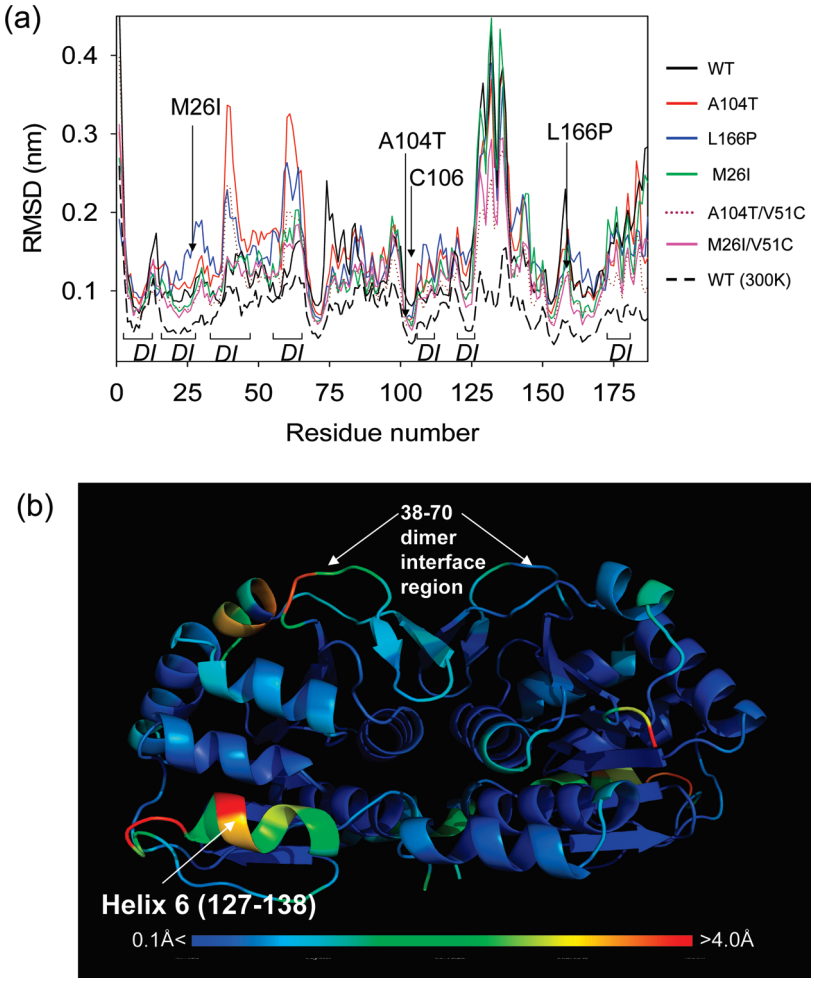

FIGURE 2: (a) Root-mean-square deviation per residue for the Cα atom for DJ-1^{WT}, the familial Parkinson's disease mutants, and their disulfide versions DJ-1$^{M26I/V51C}$ and DJ-1$^{A104T/V51C}$ observed over the course of a 1000 ps MD simulation. The maximum variability between WT and the various mutants is observed between residues 38 and 70, parts of which coincide with the dimer interface and include the V51 region. Another region of the protein with high mobility includes solvent-exposed helix 6 between residues 127 and 138. Key residues important in this investigation and indicated by arrows and the dimer interface residues are indicated by *DI*. Among the mutants, DJ-1^{A104T} and DJ-1^{L166P} appear to be more perturbed than DJ-1^{M26I} around the region of residues 38−70. Simulation trajectories of the disulfide-bonded counterparts of these mutants are indicated by a brown dotted line (DJ-1$^{A104T/V51C}$) and a pink line (DJ-1$^{M26I/V51C}$). (b) Ribbon representation of DJ-1^{A104T} representing the molecular motions in the various parts of the protein. The per-residue root-mean-square variation of panel a was converted to *B* factors and ramped using the coloring scheme indicated below (blue, rmsd = 0.0 Å; red, rmsd = 4.0 Å). Two mobile regions including the dimer interface residues (38−70) and helix 6 (127−138) are indicated by arrows.

Materials and Methods) (*50*−*52*). Briefly, the protein samples were gradually heated from 25 to 80 °C in increments of 0.5 °C, and fluorescence from Sypro Orange was measured (emission at 570 nm). Sypro Orange (ThermoFluor) has a low quantum yield in aqueous solution but readily binds to unfolding proteins with an almost 1000-fold increase in quantum yield and, therefore, is an ideal probe for monitoring the thermal stability of a protein. Thermal melting profiles were measured from three independent PCR wells (n = 3) for each sample. DJ-1^{WT} was found to be most stable with a T_m of 65 ± 0.5 °C (Figure 1c). The familial mutants were found to be less stable than WT with DJ-1^{M26I} (T_m = 52 ± 0.5 °C) and DJ-1^{A104T} (T_m = 53 ± 0.5 °C). Compared to the familial PD mutants alone, the V51C disulfide-linked versions of the mutant DJ-1 exhibited a higher degree of thermostability (DJ-1$^{M26I/V51C}$ T_m = 57 ± 0.5 °C, and DJ-1$^{A104T/V51C}$ T_m = 58 ± 0.5 °C) (Figure 1c). Thermal stabilization upon introduction of disulfide bonds to similar degrees has been reported for other protein systems as well (*53*−*55*).

Disulfide Linkages Restore Antioxidant-like Function in DJ-1 Harboring Familial Mutations. Because the disulfide linkages could effectively stabilize mutant DJ-1, we attempted to demonstrate that this would also lead to restoration of a "protein function" (the real function of DJ-1 is not known) that is contingent on protein stability. As mentioned earlier, a highly reactive cysteine (Cys 106) residue is in the proximity of Glu 18, His 126, and Arg 28 and located in a unique chemical environment made up by residues from both subunits (*32*). This structural feature gives DJ-1 the ability to reduce reactive oxygen species (ROS) by undergoing self-oxidation at Cys 106 to generate a cysteinesulfenic acid (*31*). This reaction is similar in mechanism to that utilized by the glutathione peroxidase class of enzymes. However, unlike that of glutathione peroxidase, it appears to be a stoichiometric, rather than a catalytic, reaction. To assess the ability of the various familial DJ-1 mutants to reduce ROS (in this case, cumene hydroperoxide), we employed a spectrophotometric assay that takes advantage of the observed decrease in NADPH absorbance that accompanies the glutathione oxidation−reduction reaction. In our assay, the observed decrease in NADPH absorbance is directly proportional to the peroxidase activity of the sample. DJ-1 self-oxidation is not

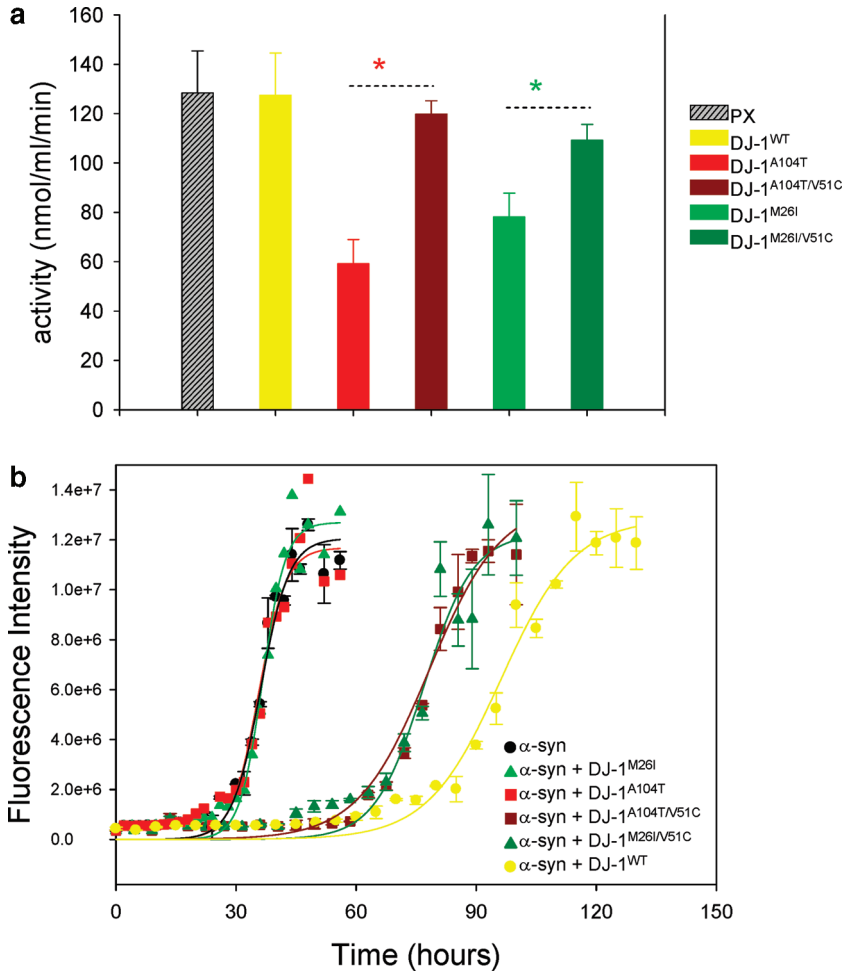

FIGURE 3: (a) Autoxidation of Cys 106 of DJ-1^{WT}, familial mutants, and disulfide-bonded (V51C) versions of the familial mutants compared using a glutathione peroxidase (PX) assay kit. Glutathione peroxidase (PX, 100 nM) was used as a positive control in this assay. The disulfide mutant DJ-$1^{A104T/V51C}$ showed an improved ability to autoxidize compared to DJ-1^{A104T} ($n = 5$, red asterisk, $p < 0.0001$, Student's t test). Similarly, DJ-$1^{M26I/V51C}$ exhibited higher glutathione peroxidase activity than DJ-1^{M26I} ($n = 5$, green asterisk, $p = 0.0004$, Student's t test). (b) Aggregation of α-synuclein in presence of DJ-1^{WT} and various mutants. Data from five independent aggregation experiments for various α-synuclein-incubated forms of DJ-1 were used for generation of the plot and error bars. α-Synuclein aggregates to completion within 48 h under our assay conditions. The mutants DJ-1^{A104T} and DJ-1^{M26I} have no effect on α-synuclein aggregation kinetics. DJ-1^{WT} delays the aggregation of α-synuclein, with the first Thio-T positive aggregates appearing around 80 h. The V51C disulfide-bonded mutants DJ-$1^{A104T/V51C}$ and DJ-$1^{A104T/V51C}$ delay the aggregation of α-synuclein, with the first Thio-T positive aggregates appearing after 60 h.

catalytic bur rather stoichiometric in nature. The various DJ-1 samples were adjusted to a concentration of 100 μM (the high concentration necessary for DJ-1^{WT} to exhibit activity comparable to the glutathione peroxidase control of 100 nM) and incubated with a cosubstrate mixture, and the absorbance was monitored at 340 nm for 30 min. Stoichiometric self-oxidation of DJ-1^{WT} and the various mutants was assessed in five independent experiments ($n = 5$), and averaged data are shown in Figure 3a. Our results show that the familial mutations DJ-1^{A104T} and DJ-1^{M26I} display a deficit in their capacity to reduce cumene hydroperoxide (Figure 3a). In contrast, their disulfide-linked mutants DJ-$1^{A104T/V51C}$ and DJ-$1^{M26I/V51C}$ were more effective in scavenging ROS in the above-mentioned assay compared to their familial mutant counterparts. This demonstrates that the stabilization of the mutants using disulfide bridges restores local structure near Cys 106 necessary for scavenging ROS.

Disulfide Linkages Rescue DJ-1's Ability To Inhibit α-Synuclein Aggregation. Wild-type DJ-1 has been shown to suppress aggregation of α-synuclein, suggesting a possible chaperone-like function for DJ-1 (*21*−*23*). This property is highly dependent on the oxidation state of DJ-1, particularly that of Cys 106 (*10*). If this is indeed true, the loss of stability in this region in the L166P, A104T, and M26I familial mutants should lead to deficits in their ability to inhibit α-synuclein fibrillization. To test this hypothesis, we measured aggregation rates for α-synuclein in the presence of the familial mutants DJ-1^{A104T} and DJ-1^{M26I}. Fibrillization of α-synuclein induced by agitation was measured by monitoring the increase in thioflavin-T fluorescence at 490 nm (details in Materials and Methods). Under agitation, samples of α-synuclein aggregated to completion in 48 h (Figure 3b). Wild-type DJ-1, added to the α-synuclein sample in equimolar quantities, slowed α-synuclein aggregation, which was in good agreement with previously published data (*23*). No aggregation of α-synuclein in the presence of DJ-1^{WT} was observed within 48 h, but the samples start to produce Thio-T positive aggregates after 80 h (Figure 3b). The implications of this result are discussed in further detail in the later sections. The addition of A104T or M26I mutant DJ-1 had no effect on the kinetics of α-synuclein aggregation. However, when introduced in equimolar concentrations into α-synuclein, oxidized samples of the double mutants DJ-$1^{A104T/V51C}$ and DJ-$1^{M26I/V51C}$ blocked the aggregation beyond 48 h but not beyond 80 h (Figure 3b). This is strong

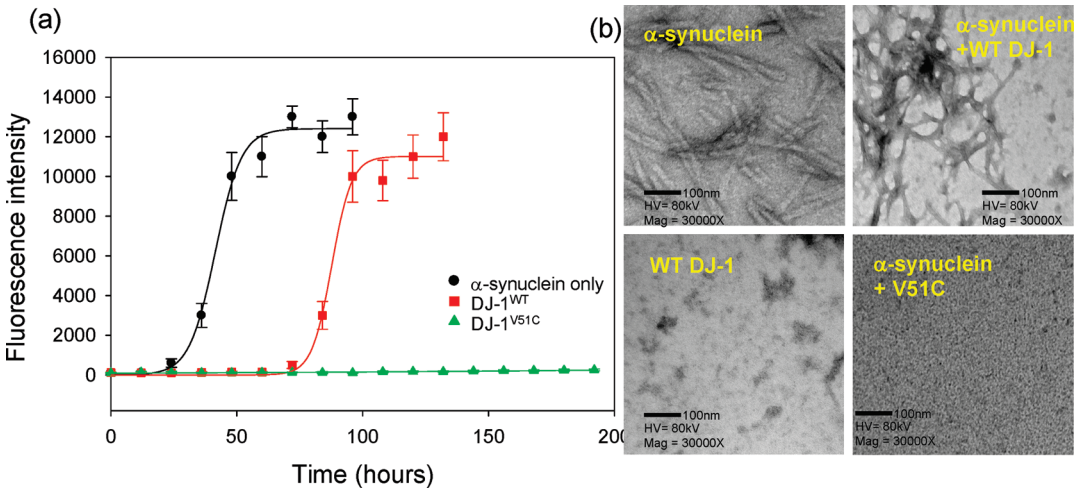

FIGURE 4: Aggregation of α-synuclein in the presence of DJ-1^{WT} and DJ-1^{V51C} followed over extended periods of time. DJ-1^{WT} is effective in blocking aggregation; however, the effect lasts only until 80 h (first Thio-T positive aggregates observed after 80 h). The disulfide-bonded DJ-1^{V51C} can exert its anti-aggregation effects for longer periods of time beyond 80 h. In this experiment, the aggregation kinetics was followed up to 196 h, during which no aggregation of α-synuclein was observed. Data from five independent aggregation assays were used to generate the plot and error bars in this study. (b) Electron microscopy analysis of mixtures of DJ-1^{WT} with α-synuclein and DJ-1^{V51C} with α-synuclein after incubation for 80 h (representative electron microscopy field shown here at 30000×). The DJ-1^{WT}/α-synuclein mixture shows both fibrillar aggregates as well as amorphous aggregates. Analysis of pure samples of α-synuclein in the control experiments shows fibrillar aggregates with amyloid-like characteristics, while DJ-1^{WT} shows amorphous aggregates.

evidence that the chaperone-like function of DJ-1 is dependent of protein stability and possibly oxidation of Cys 106. Control experiments were conducted with the reduced form of both DJ-1$^{M26I/V51C}$ and DJ-1$^{A104T/V51C}$ generated right after purification by extensive dialysis with 10 mM DTT. The assay conditions were identical to those described above. The reduced form of DJ-1$^{A104T/V51C}$ and DJ-1$^{M26I/V51C}$ did not block aggregation of α-synuclein, indicating that effect is not the mere presence of the V51C mutation but rather dependent on formation of the disulfide bond (Supplemental Figure 1b of the Supporting Information).

Disulfide-Linked Wild-Type DJ-1 Has an Enhanced Ability To Block Aggregation of α*-Synuclein*. The presence of a disulfide bond restores chaperone-like properties in the familial mutants. However, familial DJ-1 mutants represent a fairly small group in the PD patient population. On the other hand, several lines of evidence point toward a central role for the process of α-synuclein fibrillization in the etiology of PD (*56*, *57*). If wild type DJ-1 is a natural chaperone for α-synuclien, stabilization of the WT protein should lead to enhancement of its anti-aggregation properties. To test this, we conducted prolonged aggregation assays (beyond 80 h) with α-synuclein in the presence of DJ-1^{WT} and DJ-1^{V51C} (Figures 3b and 4a). Fibrillization of α-synuclein was induced by agitation in a manner similar to our previous experiments and was measured by monitoring the increase in thioflavin-T fluorescence at 490 nm (details in Materials and Methods). Under agitation, samples of α-synuclein aggregated to completion in $<$48 h (Figure 4a). In the presence of DJ-1^{WT}, no aggregation was observed until 80 h, following which there was rapid onset of α-synuclein aggregation (Figures 3b and 4a). In the presence of DJ-1^{V51C}, no aggregation was observed until 196 h, beyond which no further data points were collected. Samples containing DJ-1^{WT} and α-synuclein mixtures upon electron microscopy analysis (Figure 4b) 80 h into the assay were found to contain a mixture of amyloid fibrils presumably from α-synuclein along with amorphous protein aggregates presumably from DJ-1. Electron microscopy analysis of DJ-1^{V51C} and α-synuclein showed very few aggregated particles and no fibrillar material (Figure 4b). The DJ-1^{V51C} and α-synuclein mixture upon SDS−PAGE analysis showed the presence of both proteins and no degradation products, suggesting both samples were stable over the course of the experiment (Supplemental Figure 1c of the Supporting Information).

DISCUSSION

Since the discovery of parkin mutations, two additional genes have been found associated with recessive parkinsonism, DJ-1 (*2*) and PINK1 (*58*−*62*). Patients with mutations in either of these two genes have phenotypes similar to each other and to parkin. Onset is generally early (from age 30 to 50), and the course is benign with long disease duration. Individuals with DJ-1 mutations have loss of presynaptic dopaminergic function, although no autopsy studies are yet available. Most PD patients have either homozygous or compound heterozygous DJ-1 mutations, but some also have single heterozygous mutations, suggesting that DJ-1 loss of function accounts for disease in these individuals. The exact function of DJ-1 remains elusive, but evidence points toward functions similar to that of a free radical scavenger, a redox-dependent chaperone, or both (*23*, *63*). The presence of Cys 106 at the dimer interface of the protein in a unique chemical environment composed of charged amino acids is reminiscent of peroxidases. Indeed, Cys 106 has been shown to be readily oxidized, which presumably causes translocation of the protein to the mitochondria, where it may exert a neuroprotective effect (*27*). The mutations such as L166P, A104T, and M26I, when mapped on the crystal structure, are distant from Cys 106 but are located on secondary structural elements that make up the dimer interface and cause loss of function indirectly through a loss of structural stability (*10*). The L166P mutation is a severely destabilizing mutation, which compromises the dimeric structure of DJ-1 almost completely. Other mutations such as A104T and M26I have a weaker destabilizing effect on the protein structure. We used MD simulations to address the early structural changes that might accompany the loss of function. While proline mutations such as L166P are generally considered helix breakers, in certain cases, the overall effect of the mutation is dependent on

the position of the mutation in the helix and the surrounding residue (*64*, *65*). In a short simulation of 1000 ps to probe early events, DJ-1^{WT} was found to be stable over the course of the simulation, while DJ-1^{L166P}, DJ-1^{A104T}, and DJ-1^{M26I} were found to be less stable. Interestingly, the L166P mutation caused a mere kink in helix G, but the motion was translated to the region between residues 38 and 70 (see Figure 1b). This observation is consistent with independent simulation studies conducted by Daggett and co-workers, NMR studies conducted by Eliezer et al. (*40*), and X-ray and solvent mapping studies conducted by Ringe and co-workers (*41*). This region of the protein lies at the dimer interface and was found to be highly susceptible to unfolding in our simulations. Though essential dynamics calculations were not performed to obtain a detailed picture of the motion translation from the mutation site to the region of residues 38−70 of the protein, it was clear that the overall stability of the protein was dependent on the stability of this region. It may be argued that if the weak links in a protein that are highly susceptible to mutations are identified, they may be reinforced to prevent downstream unfolding events.

To test whether stabilization of the regions of residues 38−70 affects overall stability, residue V51 was mutated to C in the L166P, A104T, or M26I familial mutant background to generate a pair of symmetric disulfide bridges with C53 on the opposite subunit. Under oxidizing conditions, the double mutants DJ-$1^{A104T/V51C}$ and DJ-$1^{M26I/V51C}$ were found to be stabilized against thermal and chemical denaturation. DJ-1^{L166P} did not form a covalent dimer, which is consistent with the observations made by other researchers that the L166P mutation is deleterious to the structure. While DJ-1^{WT} exhibited the ability to scavenge hydroperoxide radicals and block aggregation of α-synuclein, DJ-1^{A104T} and DJ-1^{M26I} did not. This was presumably due to perturbations at the dimer interface that destroy the subtle arrangement of charged residues around Cys106 responsible for DJ-1. The double mutants DJ-$1^{A104T/V51C}$ and DJ-$1^{M26I/V51C}$ exhibited an improved ability to scavenge hydroperoxide radicals compared to their familial mutant counterparts and could effectively block the aggregation of α-synuclein, suggesting at least a partial restoration of the Cys 106 environment. An interesting observation was that the disulfide mutation in the WT background (DJ-1^{V51C}) showed a prolonged chaperone-like effect and could block aggregation of α-synuclien for extended periods of time, while DJ-1^{WT} was effective only up to 80 h. This is presumably due to the fact that any protein upon agitation unfolds, leading to the loss of function. Engineered disulfide bonds are known to make proteins more resilient to unfolding.

The strategy of native state stabilization for protein misfolding disease has been shown to be generally applicable to a number of human cases such as TTR (familial amyloidosis) (*66*), SOD-1 (Lou Gehrig's disease or ALS) (*38*, *39*), and glucocerebrosidase (Gaucher's disease) (*67*). While familial DJ-1 mutants represent a small percentage of Parkinson's patients, it may be argued that stabilization of DJ-1^{WT} with small molecules may have beneficial effects in patients with various synucleinopathies because of potentiated chaperone-like function, which may increase the degree of neuroprotection. The results described in this investigation along with those in the recent literature, in effect, validate an extensive search for druglike molecules that affect protein stability, analogous to those described in the case of TTR and SOD. Such molecules could eventually be developed into desperately needed therapeutics for Parkinson's disease.

ACKNOWLEDGMENT

We thank Dr. Peter T. Lansbury for research support and Dr. Gregory Cuny at the Laboratory for Drug Discovery in Neurodegeneration (LDDN) for useful discussions on assay design, small molecule screening, and analysis of the hits. We thank Prof. Jean-Christopher Rochet (Purdue University, West Lafayette, IN), John Hulleman (Purdue University), and Prof. Liang Tong (Columbia University, New York, NY) for providing the initial clones for human DJ-1. However, all work described here was conducted using the clones synthesized at DNA2.0. We thank Kristine Vernon for help with preparation of the manuscript.

SUPPORTING INFORMATION AVAILABLE

Ribbon diagram color-coded by the motion observed in our simulation studies, control experiments with reduced forms of the disulfide-bonded double mutants of DJ-1, and SDS−PAGE analysis of disulfide-bonded DJ-1^{V51C} and α-synuclein mixtures. This material is available free of charge via the Internet at http://pubs.acs.org.

REFERENCES

1. Dawson, T. M., and Dawson, V. L. (2003) Molecular pathways of neurodegeneration in Parkinson's disease. *Science 302*, 819–822.
2. Bonifati, V., Rizzu, P., van Baren, M. J., Schaap, O., Breedveld, G. J., Krieger, E., Dekker, M. C., Squitieri, F., Ibanez, P., Joosse, M., van Dongen, J. W., Vanacore, N., van Swieten, J. C., Brice, A., Meco, G., van Duijn, C. M., Oostra, B. A., and Heutink, P. (2003) Mutations in the DJ-1 gene associated with autosomal recessive early-onset parkinsonism. *Science 299*, 256–259.
3. Macedo, M. G., Anar, B., Bronner, I. F., Cannella, M., Squitieri, F., Bonifati, V., Hoogeveen, A., Heutink, P., and Rizzu, P. (2003) The DJ-1 L166P mutant protein associated with early onset Parkinson's disease is unstable and forms higher-order protein complexes. *Hum. Mol. Genet. 12*, 2807–2816.
4. Miller, D. W., Ahmad, R., Hague, S., Baptista, M. J., Canet-Aviles, R., McLendon, C., Carter, D. M., Zhu, P. P., Stadler, J., Chandran, J., Klinefelter, G. R., Blackstone, C., and Cookson, M. R. (2003) L166P mutant DJ-1, causative for recessive Parkinson's disease, is degraded through the ubiquitin-proteasome system. *J. Biol. Chem. 278*, 36588–36595.
5. Abou-Sleiman, P. M., Healy, D. G., Quinn, N., Lees, A. J., and Wood, N. W. (2003) The role of pathogenic DJ-1 mutations in Parkinson's disease. *Ann. Neurol. 54*, 283–286.
6. Hering, R., Strauss, K. M., Tao, X., Bauer, A., Woitalla, D., Mietz, E. M., Petrovic, S., Bauer, P., Schaible, W., Muller, T., Schols, L., Klein, C., Berg, D., Meyer, P. T., Schulz, J. B., Wollnik, B., Tong, L., Kruger, R., and Riess, O. (2004) Novel homozygous p.E64D mutation in DJ1 in early onset Parkinson disease (PARK7). *Hum. Mutat. 24*, 321–329.
7. Annesi, G., Savettieri, G., Pugliese, P., D'Amelio, M., Tarantino, P., Ragonese, P., La Bella, V., Piccoli, T., Civitelli, D., Annesi, F., Fierro, B., Piccoli, F., Arabia, G., Caracciolo, M., Ciro Candiano, I. C., and Quattrone, A. (2005) DJ-1 mutations and parkinsonism-dementia-amyotrophic lateral sclerosis complex. *Ann. Neurol. 58*, 803–807.
8. Hague, S., Rogaeva, E., Hernandez, D., Gulick, C., Singleton, A., Hanson, M., Johnson, J., Weiser, R., Gallardo, M., Ravina, B., Gwinn-Hardy, K., Crawley, A., St George-Hyslop, P. H., Lang, A. E., Heutink, P., Bonifati, V., and Hardy, J. (2003) Early-onset Parkinson's disease caused by a compound heterozygous DJ-1 mutation. *Ann. Neurol. 54*, 271–274.
9. Clark, L. N., Afridi, S., Mejia-Santana, H., Harris, J., Louis, E. D., Cote, L. J., Andrews, H., Singleton, A., Wavrant De-Vrieze, F., Hardy, J., Mayeux, R., Fahn, S., Waters, C., Ford, B., Frucht, S., Ottman, R., and Marder, K. (2004) Analysis of an early-onset Parkinson's disease cohort for DJ-1 mutations. *Mov. Disord. 19*, 796–800.
10. Lakshminarasimhan, M., Maldonado, M. T., Zhou, W., Fink, A. L., and Wilson, M. A. (2008) Structural impact of three Parkinsonism-associated missense mutations on human DJ-1. *Biochemistry 47*, 1381–1392.
11. Nagakubo, D., Taira, T., Kitaura, H., Ikeda, M., Tamai, K., Iguchi-Ariga, S. M., and Ariga, H. (1997) DJ-1, a novel oncogene which

transforms mouse NIH3T3 cells in cooperation with ras. *Biochem. Biophys. Res. Commun. 231*, 509–513.
12. Klinefelter, G. R., Laskey, J. W., Ferrell, J., Suarez, J. D., and Roberts, N. L. (1997) Discriminant analysis indicates a single sperm protein (SP22) is predictive of fertility following exposure to epididymal toxicants. *J. Androl. 18*, 139–150.
13. Aleyasin, H., Rousseaux, M. W., Phillips, M., Kim, R. H., Bland, R. J., Callaghan, S., Slack, R. S., During, M. J., Mak, T. W., and Park, D. S. (2007) The Parkinson's disease gene DJ-1 is also a key regulator of stroke-induced damage. *Proc. Natl. Acad. Sci. U.S.A. 104*, 18748–18753.
14. Shinbo, Y., Taira, T., Niki, T., Iguchi-Ariga, S. M., and Ariga, H. (2005) DJ-1 restores p53 transcription activity inhibited by Topors/p53BP3. *Int. J. Oncol. 26*, 641–648.
15. Taira, T., Iguchi-Ariga, S. M., and Ariga, H. (2004) Co-localization with DJ-1 is essential for the androgen receptor to exert its transcription activity that has been impaired by androgen antagonists. *Biol. Pharm. Bull. 27*, 574–577.
16. Takahashi, K., Taira, T., Niki, T., Seino, C., Iguchi-Ariga, S. M., and Ariga, H. (2001) DJ-1 positively regulates the androgen receptor by impairing the binding of PIASx α to the receptor. *J. Biol. Chem. 276*, 37556–37563.
17. Zhong, N., Kim, C. Y., Rizzu, P., Geula, C., Porter, D. R., Pothos, E. N., Squitieri, F., Heutink, P., and Xu, J. (2006) DJ-1 transcriptionally up-regulates the human tyrosine hydroxylase by inhibiting the sumoylation of pyrimidine tract-binding protein-associated splicing factor. *J. Biol. Chem. 281*, 20940–20948.
18. Hod, Y., Pentyala, S. N., Whyard, T. C., and El-Maghrabi, M. R. (1999) Identification and characterization of a novel protein that regulates RNA-protein interaction. *J. Cell. Biochem. 72*, 435–444.
19. Shinbo, Y., Niki, T., Taira, T., Ooe, H., Takahashi-Niki, K., Maita, C., Seino, C., Iguchi-Ariga, S. M., and Ariga, H. (2006) Proper SUMO-1 conjugation is essential to DJ-1 to exert its full activities. *Cell Death Differ. 13*, 96–108.
20. Kim, R. H., Peters, M., Jang, Y., Shi, W., Pintilie, M., Fletcher, G. C., DeLuca, C., Liepa, J., Zhou, L., Snow, B., Binari, R. C., Manoukian, A. S., Bray, M. R., Liu, F. F., Tsao, M. S., and Mak, T. W. (2005) DJ-1, a novel regulator of the tumor suppressor PTEN. *Cancer Cell 7*, 263–273.
21. Batelli, S., Albani, D., Rametta, R., Polito, L., Prato, F., Pesaresi, M., Negro, A., and Forloni, G. (2008) DJ-1 modulates α-synuclein aggregation state in a cellular model of oxidative stress: Relevance for Parkinson's disease and involvement of HSP70. *PLoS One 3*, e1884.
22. Li, H. M., Niki, T., Taira, T., Iguchi-Ariga, S. M., and Ariga, H. (2005) Association of DJ-1 with chaperones and enhanced association and colocalization with mitochondrial Hsp70 by oxidative stress. *Free Radical Res. 39*, 1091–1099.
23. Zhou, W., Zhu, M., Wilson, M. A., Petsko, G. A., and Fink, A. L. (2006) The oxidation state of DJ-1 regulates its chaperone activity toward alpha-synuclein. *J. Mol. Biol. 356*, 1036–1048.
24. Wei, Y., Ringe, D., Wilson, M. A., and Ondrechen, M. J. (2007) Identification of functional subclasses in the DJ-1 superfamily proteins. *PLoS Comput. Biol. 3*, e10.
25. Lee, S. J., Kim, S. J., Kim, I. K., Ko, J., Jeong, C. S., Kim, G. H., Park, C., Kang, S. O., Suh, P. G., Lee, H. S., and Cha, S. S. (2003) Crystal structures of human DJ-1 and *Escherichia coli* Hsp31, which share an evolutionarily conserved domain. *J. Biol. Chem. 278*, 44552–44559.
26. Kinumi, T., Kimata, J., Taira, T., Ariga, H., and Niki, E. (2004) Cysteine-106 of DJ-1 is the most sensitive cysteine residue to hydrogen peroxide-mediated oxidation in vivo in human umbilical vein endothelial cells. *Biochem. Biophys. Res. Commun. 317*, 722–728.
27. Canet-Aviles, R. M., Wilson, M. A., Miller, D. W., Ahmad, R., McLendon, C., Bandyopadhyay, S., Baptista, M. J., Ringe, D., Petsko, G. A., and Cookson, M. R. (2004) The Parkinson's disease protein DJ-1 is neuroprotective due to cysteine-sulfinic acid-driven mitochondrial localization. *Proc. Natl. Acad. Sci. U.S.A. 101*, 9103–9108.
28. Krebiehl, G., Ruckerbauer, S., Burbulla, L. F., Kieper, N., Maurer, B., Waak, J., Wolburg, H., Gizatullina, Z., Gellerich, F. N., Woitalla, D., Riess, O., Kahle, P. J., Proikas-Cezanne, T., and Kruger, R. (2010) Reduced basal autophagy and impaired mitochondrial dynamics due to loss of Parkinson's disease-associated protein DJ-1. *PLoS One 5*, e9367.
29. Scherz-Shouval, R., and Elazar, Z. (2007) ROS, mitochondria and the regulation of autophagy. *Trends Cell Biol. 17*, 422–427.
30. Kim, I., Rodriguez-Enriquez, S., and Lemasters, J. J. (2007) Selective degradation of mitochondria by mitophagy. *Arch. Biochem. Biophys. 462*, 245–253.
31. Witt, A. C., Lakshminarasimhan, M., Remington, B. C., Hasim, S., Pozharski, E., and Wilson, M. A. (2008) Cysteine pKa depression by a protonated glutamic acid in human DJ-1. *Biochemistry 47*, 7430–7440.
32. Wilson, M. A., Collins, J. L., Hod, Y., Ringe, D., and Petsko, G. A. (2003) The 1.1-Å resolution crystal structure of DJ-1, the protein mutated in autosomal recessive early onset Parkinson's disease. *Proc. Natl. Acad. Sci. U.S.A. 100*, 9256–9261.
33. Hulleman, J. D., Mirzaei, H., Guigard, E., Taylor, K. L., Ray, S. S., Kay, C. M., Regnier, F. E., and Rochet, J. C. (2007) Destabilization of DJ-1 by familial substitution and oxidative modifications: Implications for Parkinson's disease. *Biochemistry 46*, 5776–5789.
34. Gorner, K., Holtorf, E., Waak, J., Pham, T. T., Vogt-Weisenhorn, D. M., Wurst, W., Haass, C., and Kahle, P. J. (2007) Structural determinants of the C-terminal helix-kink-helix motif essential for protein stability and survival promoting activity of DJ-1. *J. Biol. Chem. 282*, 13680–13691.
35. Blackinton, J., Ahmad, R., Miller, D. W., van der Brug, M. P., Canet-Aviles, R. M., Hague, S. M., Kaleem, M., and Cookson, M. R. (2005) Effects of DJ-1 mutations and polymorphisms on protein stability and subcellular localization. *Brain Res. Mol. Brain Res. 134*, 76–83.
36. Moore, D. J., Zhang, L., Troncoso, J., Lee, M. K., Hattori, N., Mizuno, Y., Dawson, T. M., and Dawson, V. L. (2005) Association of DJ-1 and parkin mediated by pathogenic DJ-1 mutations and oxidative stress. *Hum. Mol. Genet. 14*, 71–84.
37. Adamski-Werner, S. L., Palaninathan, S. K., Sacchettini, J. C., and Kelly, J. W. (2004) Diflunisal analogues stabilize the native state of transthyretin. Potent inhibition of amyloidogenesis. *J. Med. Chem. 47*, 355–374.
38. Ray, S. S., Nowak, R. J., Strokovich, K., Brown, R. H., Jr., Walz, T., and Lansbury, P. T., Jr. (2004) An intersubunit disulfide bond prevents in vitro aggregation of a superoxide dismutase-1 mutant linked to familial amytrophic lateral sclerosis. *Biochemistry 43*, 4899–4905.
39. Ray, S. S., Nowak, R. J., Brown, R. H., Jr., and Lansbury, P. T., Jr. (2005) Small-molecule-mediated stabilization of familial amyotrophic lateral sclerosis-linked superoxide dismutase mutants against unfolding and aggregation. *Proc. Natl. Acad. Sci. U.S.A. 102*, 3639–3644.
40. Malgieri, G., and Eliezer, D. (2008) Structural effects of Parkinson's disease linked DJ-1 mutations. *Protein Sci. 17*, 855–868.
41. Landon, M. R., Lieberman, R. L., Hoang, Q. Q., Ju, S., Caaveiro, J. M., Orwig, S. D., Kozakov, D., Brenke, R., Chuang, G. Y., Beglov, D., Vajda, S., Petsko, G. A., and Ringe, D. (2009) Detection of ligand binding hot spots on protein surfaces via fragment-based methods: Application to DJ-1 and glucocerebrosidase. *J. Comput.-Aided Mol. Des.,* 491–500.
42. Anderson, P. C., and Daggett, V. (2008) Molecular basis for the structural instability of human DJ-1 induced by the L166P mutation associated with Parkinson's disease. *Biochemistry 47*, 9380–9393.
43. Van Der Spoel, D., Lindahl, E., Hess, B., Groenhof, G., Mark, A. E., and Berendsen, H. J. (2005) GROMACS: Fast, flexible, and free. *J. Comput. Chem. 26*, 1701–1718.
44. Bjork, A., Dalhus, B., Mantzilas, D., Eijsink, V. G., and Sirevag, R. (2003) Stabilization of a tetrameric malate dehydrogenase by introduction of a disulfide bridge at the dimer-dimer interface. *J. Mol. Biol. 334*, 811–821.
45. Zavialov, A., Benndorf, R., Ehrnsperger, M., Zav'yalov, V., Dudich, I., Buchner, J., and Gaestel, M. (1998) The effect of the intersubunit disulfide bond on the structural and functional properties of the small heat shock protein Hsp25. *Int. J. Biol. Macromol. 22*, 163–173.
46. Gokhale, R. S., Ray, S. S., Balaram, H., and Balaram, P. (1999) Unfolding of *Plasmodium falciparum* triosephosphate isomerase in urea and guanidinium chloride: Evidence for a novel disulfide exchange reaction in a covalently cross-linked mutant. *Biochemistry 38*, 423–431.
47. MacDonald, J. T., Purkiss, A. G., Smith, M. A., Evans, P., Goodfellow, J. M., and Slingsby, C. (2005) Unfolding crystallins: The destabilizing role of a β-hairpin cysteine in βB2-crystallin by simulation and experiment. *Protein Sci. 14*, 1282–1292.
48. Tao, X., and Tong, L. (2003) Crystal structure of human DJ-1, a protein associated with early onset Parkinson's disease. *J. Biol. Chem. 278*, 31372–31379.
49. Dombkowski, A. A. (2003) Disulfide by Design: A computational method for the rational design of disulfide bonds in proteins. *Bioinformatics 19*, 1852–1853.
50. Ericsson, U. B., Hallberg, B. M., Detitta, G. T., Dekker, N., and Nordlund, P. (2006) Thermofluor-based high-throughput stability optimization of proteins for structural studies. *Anal. Biochem. 357*, 289–298.

51. Mezzasalma, T. M., Kranz, J. K., Chan, W., Struble, G. T., Schalk-Hihi, C., Deckman, I. C., Springer, B. A., and Todd, M. J. (2007) Enhancing recombinant protein quality and yield by protein stability profiling. *J. Biomol. Screening 12*, 418–428.
52. Cummings, M. D., Farnum, M. A., and Nelen, M. I. (2006) Universal screening methods and applications of ThermoFluor. *J. Biomol. Screening 11*, 854–863.
53. Jacobson, R. H., Matsumura, M., Faber, H. R., and Matthews, B. W. (1992) Structure of a stabilizing disulfide bridge mutant that closes the active-site cleft of T4 lysozyme. *Protein Sci. 1*, 46–57.
54. Gokhale, R. S., Agarwalla, S., Francis, V. S., Santi, D. V., and Balaram, P. (1994) Thermal stabilization of thymidylate synthase by engineering two disulfide bridges across the dimer interface. *J. Mol. Biol. 235*, 89–94.
55. Velanker, S. S., Gokhale, R. S., Ray, S. S., Gopal, B., Parthasarathy, S., Santi, D. V., Balaram, P., and Murthy, M. R. (1999) Disulfide engineering at the dimer interface of *Lactobacillus casei* thymidylate synthase: Crystal structure of the T155C/E188C/C244T mutant. *Protein Sci. 8*, 930–933.
56. Conway, K. A., Harper, J. D., and Lansbury, P. T., Jr. (2000) Fibrils formed in vitro from α-synuclein and two mutant forms linked to Parkinson's disease are typical amyloid. *Biochemistry 39*, 2552–2563.
57. Caughey, B., and Lansbury, P. T. (2003) Protofibrils, pores, fibrils, and neurodegeneration: Separating the responsible protein aggregates from the innocent bystanders. *Annu. Rev. Neurosci. 26*, 267–298.
58. Yang, Y. X., Wood, N. W., and Latchman, D. S. (2009) Molecular basis of Parkinson's disease. *NeuroReport 20*, 150–156.
59. Biskup, S., Gerlach, M., Kupsch, A., Reichmann, H., Riederer, P., Vieregge, P., Wullner, U., and Gasser, T. (2008) Genes associated with Parkinson syndrome. *J. Neurol. 255* (Suppl. 5), 8–17.
60. Bonifati, V. (2007) Genetics of parkinsonism. *Parkinsonism Relat. Disord. 13* (Suppl. 3), S233–S241.
61. da Costa, C. A. (2007) DJ-1: A newcomer in Parkinson's disease pathology. *Curr. Mol. Med. 7*, 650–657.
62. Dodson, M. W., and Guo, M. (2007) Pink1, Parkin, DJ-1 and mitochondrial dysfunction in Parkinson's disease. *Curr. Opin. Neurobiol. 17*, 331–337.
63. Shendelman, S., Jonason, A., Martinat, C., Leete, T., and Abeliovich, A. (2004) DJ-1 is a redox-dependent molecular chaperone that inhibits α-synuclein aggregate formation. *PLoS Biol. 2*, e362.
64. Li, S. C., Goto, N. K., Williams, K. A., and Deber, C. M. (1996) α-Helical, but not β-sheet, propensity of proline is determined by peptide environment. *Proc. Natl. Acad. Sci. U.S.A. 93*, 6676–6681.
65. Chakrabarti, P., and Chakrabarti, S. (1998) C−H···O hydrogen bond involving proline residues in α-helices. *J. Mol. Biol. 284*, 867–873.
66. Hammarstrom, P., Wiseman, R. L., Powers, E. T., and Kelly, J. W. (2003) Prevention of transthyretin amyloid disease by changing protein misfolding energetics. *Science 299*, 713–716.
67. Lieberman, R. L., Wustman, B. A., Huertas, P., Powe, A. C., Jr., Pine, C. W., Khanna, R., Schlossmacher, M. G., Ringe, D., and Petsko, G. A. (2007) Structure of acid β-glucosidase with pharmacological chaperone provides insight into Gaucher disease. *Nat. Chem. Biol. 3*, 101–107.